SUPPORTING INFORMATION

Self-Powered Temperature Sensor with Seebeck Effect Transduction for Photothermal-Thermoelectric Coupled Immunoassay

Lingting Huang, Jialun Chen, Zhonghua Yu, and Dianping Tang*

Key Laboratory of Analytical Science for Food Safety and Biology (MOE & Fujian Province), Department of Chemistry, Fuzhou University, Fuzhou 350108, People's Republic of China

CORRESPONDING AUTHOR INFORMATION

Phone: +86-591-2286 6125; fax: +86-591-2286 6135; e-mail: dianping.tang@fzu.edu.cn (D. Tang)

TABLE OF CONTENTS

EXPERIMENTAL SECTION

Buffers. A pH 9.6 coating buffer (1.59 g Na_2CO_3, 2.93 g $NaHCO_3$, and 0.2 g NaN_3) was prepared by adding the chemicals to 1000-mL distilled water. The blocking buffer and washing buffer were obtained by the addition of 1.0% BSA (w/v) and 0.05% Tween 20 (v/v) into pH 7.4 PBS (0.01 M), respectively.

Apparatus. The scanning electron microscope (SEM) characterizations were performed on the JSM-6700 F field emission scanning electron microscope. UV-vis absorption spectra were recorded by the Infinite M200 Pro NanoQuant, (Tecan, Switzerland). Raman spectroscopy (Renishaw, 532 nm solid laser, U.K.) were recorded to further confirm the molecular structures. All electrochemical measurements were performed on CHI850D Electrochemical Workstation (Shanghai Chenhua Inc., China). The current analysis detection was using a digital multimeter (VC9801A+, VICTOR). The vessel and mold were printed by a 3D printer (Formlabs2, USA). X-ray photoelectron spectra (XPS) was obtained from ESCALAB 250Xi (Thermo-VG Scientific Co., Ltd). Field scanning electron Microscopy (FSEM) was executed on Nova NanoSEM 230 (FEI Czech Republc S.R.O. Co., Ltd). Laser power meter LP1 (Sanwa, Japan) was used to measure the optical power.

Immunoreaction and Photothermal-Thermoelectric Measurement on a Portable Digital Multimeter. The process of the sandwich-type immunoassay was shown in Scheme S1. Prior to measurement, 100 μL of mouse anti-AFP mAb (5 μg mL^{-1}, correspond to the "capture antibody") was added to the wells of a 96-well microtiter plate and incubated at 4 °C for 12 h. After being washed by washing buffer (PBS containing 0.05 wt % tween 20) for three times, the wells were blocked by 200 μL of blocking buffer (PBS containing 0.05 wt % tween 20 and 2.0 wt % BSA) and incubated at 37 °C for 1 h. Then, the wells were washed three times by washing buffer, followed by addition of 100 μL of AFP standards in dilution buffer (PBS containing 0.05 wt % tween 20 and 0.5 wt % BSA). After being shaken on a shaker at room temperature for 1 h, the wells were washed by washing buffer for three times. 100 μL of rabbit anti-AFP pAb (2.0 μg mL^{-1}, correspond to the "detection antibody") was added to the wells, followed by shaking at room temperature for 1 h. After the wells had been washed three times by washing buffer, 100 μL of GOx-goat anti-rabbit IgG conjugates diluent was added, followed by 1 h shaking at room temperature. After three times

washing by washing buffer, 220 μL of pH 5.0 PBS containing 50 mM glucose was added into each well and reacted for 20 min at 37 °C. After that, 200 μL of the reaction solution including H_2O_2 was mixed with 200 μL of TMB substrate solution (100 μL of 12mM TMB and 50 μL of 1 mg mL^{-1} HRP in 50 μL of pH 5.0 PBS) and reacted for 20 min at room temperature (25 ± 1.0 °C). Then, 390 μL of the reaction fluid was transferred to a sample pool and irradiated with the 808-nm laser at 0.8 W and then recorded the open-circuit voltage generated by the thermoelectric module. All the data were obtained with three measurements each in parallel.

Immunoreaction and Photothermal Measurement on a Portable Digital Thermometer. Scheme S1 gives the schematic illustration of sandwich-type immunoassay toward target AFP in the microplate by using GOx as the signal-transduction tags with a portable digital thermometer. Prior to measurement, 100 μL of mouse anti-AFP capture antibody (5 μg mL^{-1}) was added to the wells of a 96-well microtiter plate and incubated at 4 °C for 12 h. After being washed by washing buffer (PBS containing 0.05 wt % tween 20) for three times, the wells were blocked by 200 μL of blocking buffer (PBS containing 0.05 wt % tween 20 and 2.0 wt % BSA) and incubated at 37 °C for 1 h. Then, the wells were washed three times by washing buffer, followed by addition of 100 μL of AFP standards in dilution buffer (PBS containing 0.05 wt % tween 20 and 0.5 wt % BSA). After being shaken on a shaker at room temperature for 1 h, the wells were washed by washing buffer for three times. 100 μL of rabbit anti-AFP detection antibody (2.0 μg mL^{-1}) was added to the wells, followed by shaking at room temperature for 1 h. After the wells had been washed three times by washing buffer, 100 μL of GOx-goat anti-rabbit IgG conjugates diluent was added, followed by 1 h shaking at room temperature. After three times washing by washing buffer, 220 μL of pH 5.0 PBS containing 50 mM glucose was added into each well and reacted for 20 min at 37 °C. After that, the resulting solution including the as-produced H_2O_2 was mixed with 220 μL of TMB substrate solution (100 μL of 12mM TMB and 50 μL of 1 mg mL^{-1} HRP in 50 μL of pH 5.0 PBS) and reacted for 20 min at room temperature (25 ± 1.0 °C). Subsequently, the temperature sensor was inserted into the microplate (close to the bottom of the well), and the temperature of the detection solution was determined by coupling with TMB-H_2O_2-based photo-heat conversion system on a portable digital thermometer (VICTOR 6801, Double King Industrial Holdings Co., Ltd., Shenzhen, China; www.china-victor.com) under an 808-nm adjustable laser irradiation (0.8 W) (Scheme S1). The collected temperature relative to target AFP concentration was recorded as signal of photothermal

immunoassay. All the determinations were made at least in duplicate. All the measurements were carried out at room temperature (25 ± 1.0 °C), unless special statement.

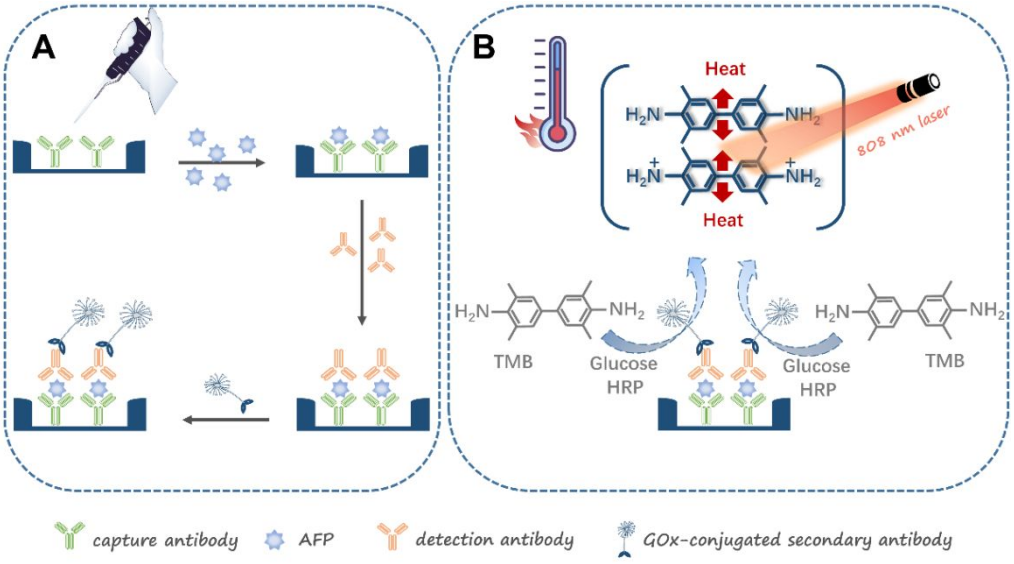

Scheme S1. (A) Schematic illustration of the sandwich-type immunoreaction protocol, and (B) production of photothermal solution.

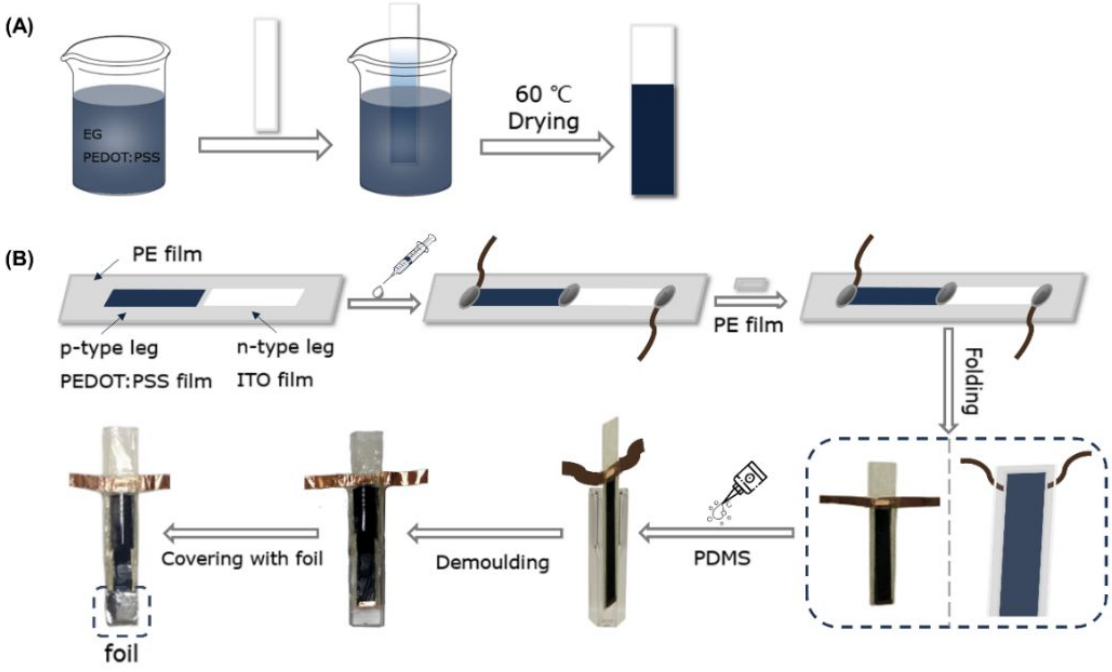

Scheme S2. Fabrication process of (A) the flexible *p*-type leg and (B) folding-designed thermoelectric module.

PARTIAL RESULTS AND DISCUSSION

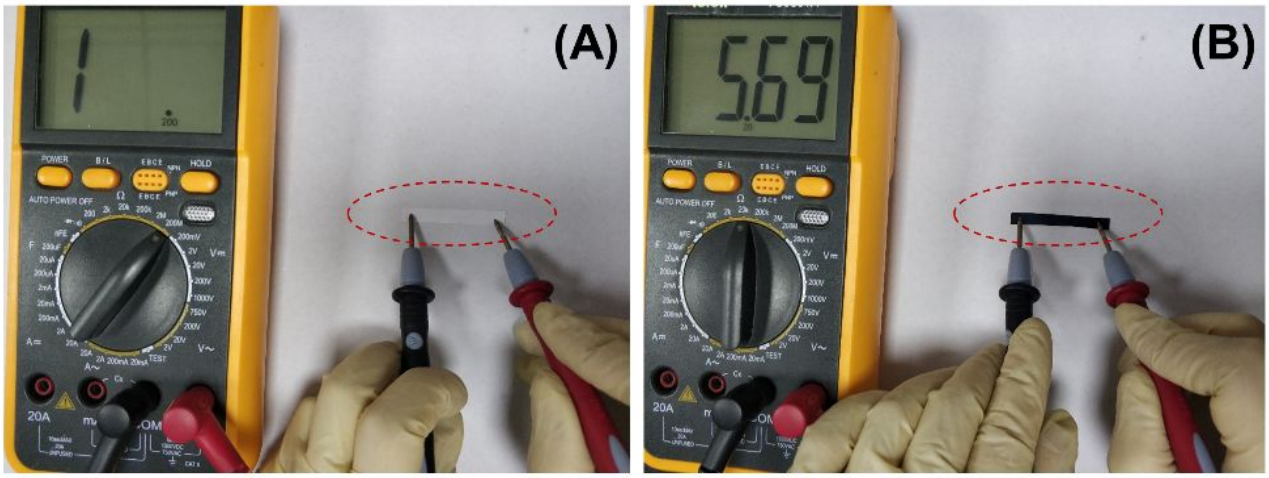

Figure S1. Photographs of the change in electrical conductivity (A) before and (B) after soaking PEDOT:PSS solution.

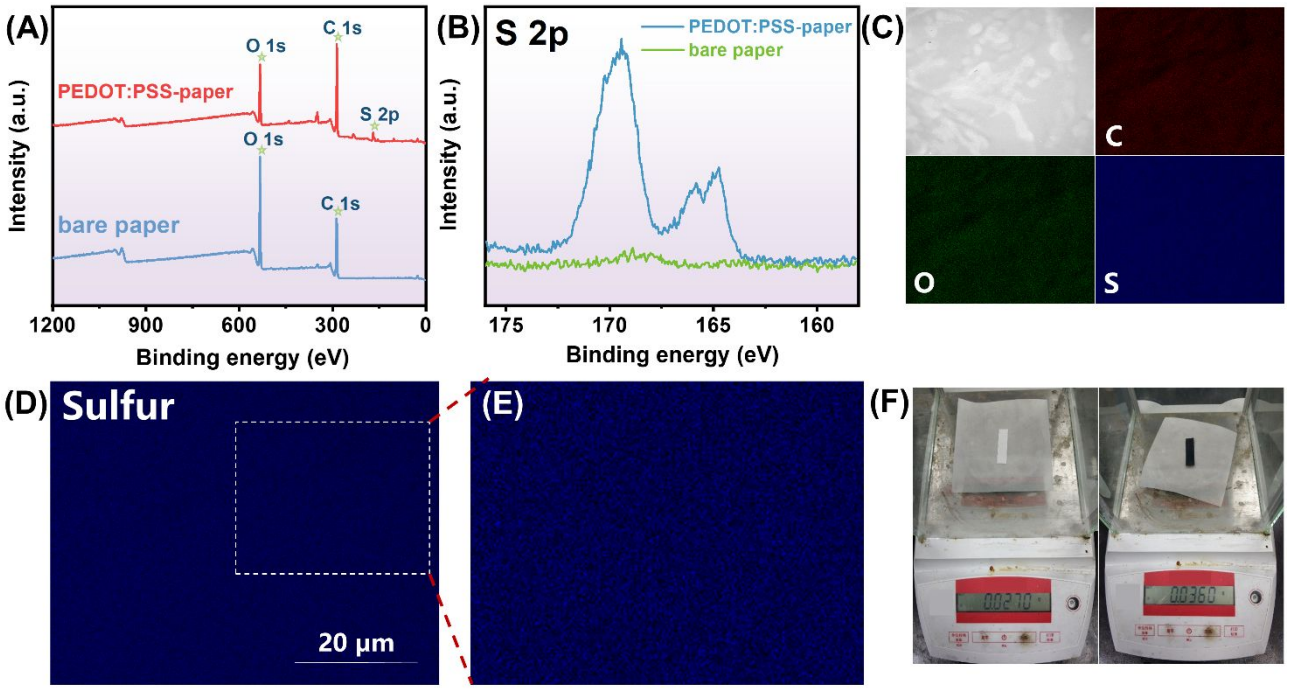

Figure S2. (A) XPS spectra and (B) S 2p spectra of bare paper and PEDOT:PSS-paper; (C) FSEM image and element mapping for O (green), C (red), and S (blue) of PEDOT:PSS-paper; (D) Element mapping of the sulfur within the PEDOT:PSS-paper and (E) the corresponding magnification image; (F) Weight comparison of paper before and after soaking PEDOT:PSS solution (the one on the left is bare paper, and the one on the right is PEDOT:PSS-paper).

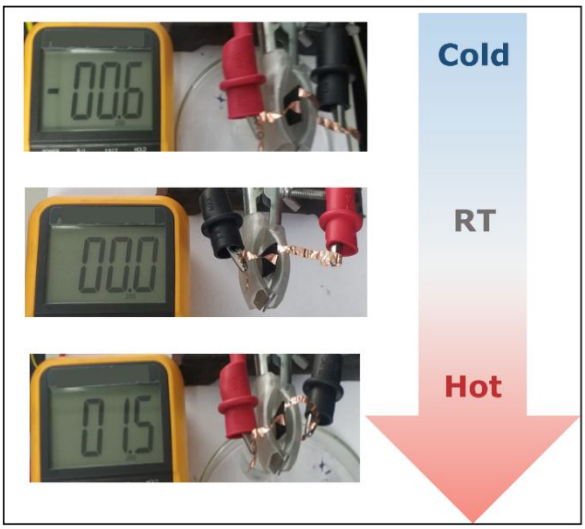

Figure S3. Demonstrations of the flexible thermoelectric module through digital multimeter.

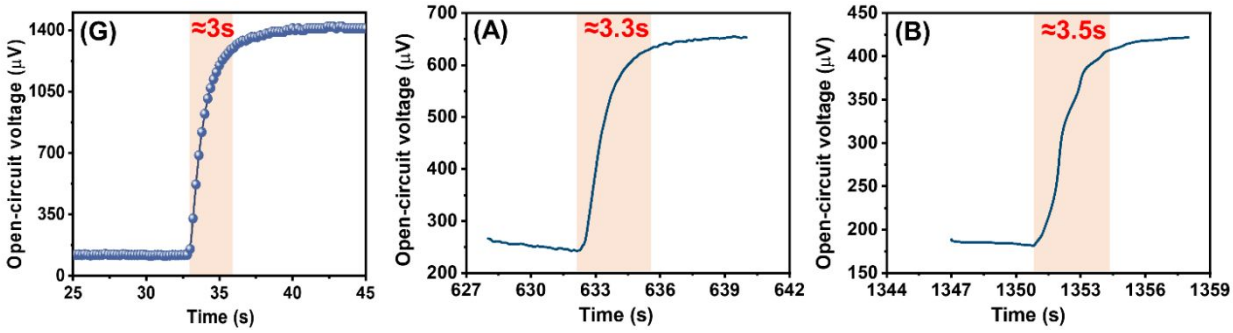

Figure S4. Response times at different temperatures (A) 60 ºC, (B) 45 ºC, and (C) 30 ºC.

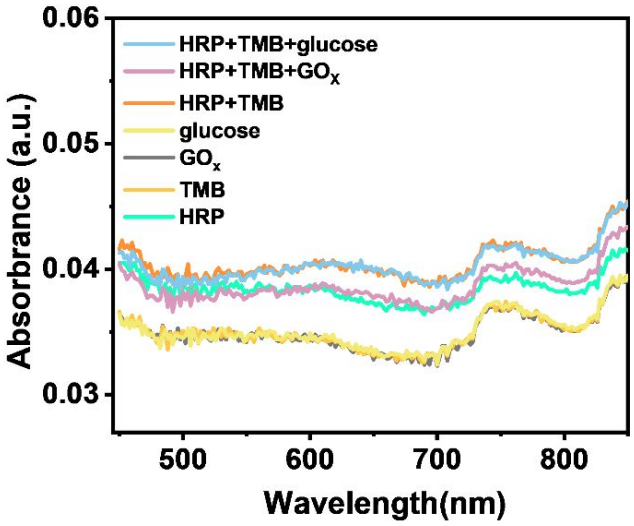

Figure S5. The magnification image of UV-vis absorption spectra of different components including HRP, TMB, GOx, glucose, HRP + TMB, HRP + TMB + GOx and HRP + TMB + glucose.

Figure S6. Photothermal contrast images and photographs of different solutions corresponding to (1) HRP, (2) TMB, (3) GOx, (4) glucose, (5) HRP and TMB, (6) HRP, TMB and GOx, (7) HRP, TMB and glucose, (8) HRP, TMB, GOx and glucose.

Optimization of Experimental Conditions. To optimize the analytical performance of the proposed testing, several possible experimental parameters influencing the detection result should be investigated, including irradiation time, colorimetric reaction time, and HRP concentration, As indicated in Figure S7-A, the open-circuit voltage initially increased with the increasing irradiation time, and then tended to level off after 600 s, and the slope of the corresponding curve also approaches 0 (30 ng mL^{-1} AFP used in this case). To shorten the assay time, 600 s of irradiation time was chosen. By the same token, we also monitored the effect of colorimetric reaction time. As shown in Figure S7-B, the changing value of open-circuit voltage change increased gradually and remained to a steady value after 10 min. But in order to get a thorough reaction, 20 min was utilized as the colorimetric reaction time. To better illustrate the optimal reaction time, we explored the relationship between the changing value of open-circuit voltage and time for each set of parallel samples in Figure S7-D. As shown in Figure S7-D, analogically, the changing value of open-circuit voltage increased with the reaction time, then arrived at a platform sufficiently after 20 min. More time to reaction did not bring about an obvious open-circuit voltage increasing. Therefore, 20 min was selected for producing the photothermal product in this work. Moreover, the concentration of HRP in solution was also studied. Since the light absorption of the solution can indirectly reflect the

photothermal absorption capacity of the solution, the UV-vis absorption spectra of the substrate solution containing different HRP was collected in the experiment. As depicted in Figure S7-C, the detectable signals first elevated with the increment of HRP concentrations and then reached a plateau and excess HRP concentrations did not cause a significant increase in the photocurrent. To save the detection cost, HRP concentration of 1.0 mg mL^{-1} was employed.

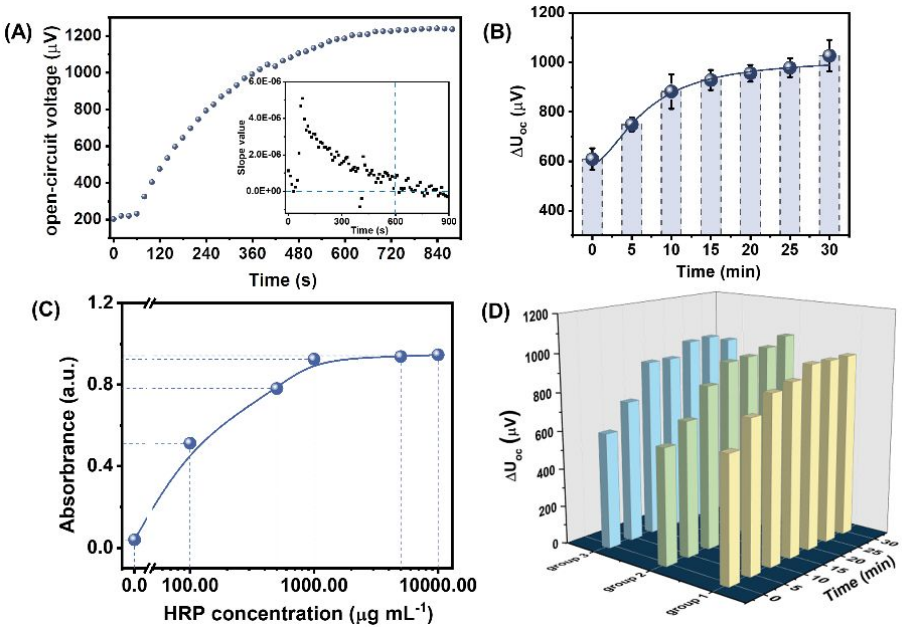

Figure S7. Influence of (A) irradiation time, (B) colorimetric reaction time, (C) HRP concentration in substrate solution, and (D) the trend graph of three parallel samples in the experiment of optimizing colorimetric reaction time.

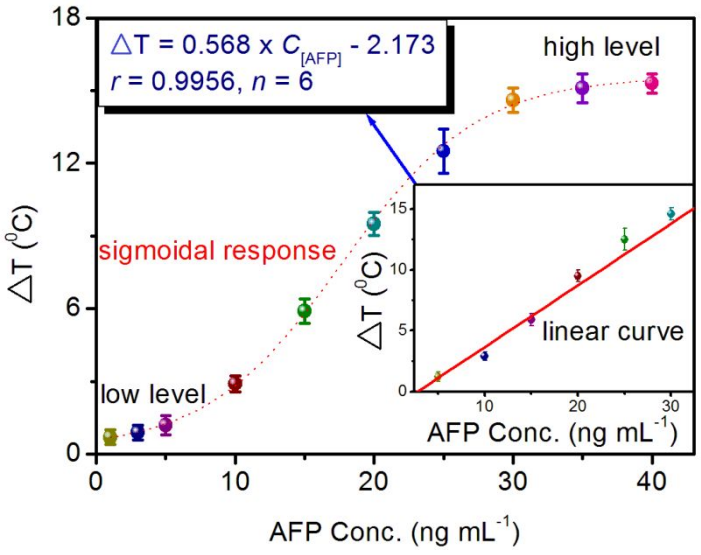

Figure S8. Calibration plots of photothermal immunoassay on a digital thermometer between the temperature shift (ΔT, °C) and CA 19-9 level (inset: linear curve).

Figure S9. Photos of the laser power meter under (A) electric light environment without foil wrapping, (B) electric light environment with foil wrapping, (C) NIR laser with foil wrapping.

In order to better verify that the integrated detection device can effectively avoid the influence of light, we first prove that the foil can effectively block surrounding light. When the laser power meter did not covered with foil, the ambient light power received by the optical sensor was 0.7 mW. When the detector was wrapped on foil, neither ambient light nor infrared light can be detected through the foil. At this time, the optical power meter read 0 mW (Figure S9).

To compensate the variation caused by ambient temperature, ΔU_{oc}, the absolute increment value of open-circuit voltage of immunoassay solutions calculated by equation ($\Delta U_{oc} = U - U_0$, where U and U_0 represent the measurable open-circuit voltage and the open-circuit voltage under surrounding temperature, respectively) was used for linear fitting. In addition, the stability of the integrated detection device in different surrounding light was also detected. Since the sample cuvette in the integrated detection device was designed to be placed in a light-tight card slot, this provides a condition for the sensor to have the ability to avoid ambient light. As shown in Figure S10-A, there is no significant difference in AFP detection under sunlight, electric light and darkroom conditions. On the other hand, the sample cuvette was well wrapped by the insulating cotton in order to avoid temperature loss and transmission. We know that the adjustable temperature range of the air conditioner is usually between 16-30 °C, so we further change the indoor ambient temperature through the air conditioner, and explore the difference of the AFP detection of the sensor under the condition of 16, 20, 25, 30 °C. Figure S10-B was added to show that there is no significant difference in detecting AFP even if the ambient temperature crosses from 16 to 30 °C.

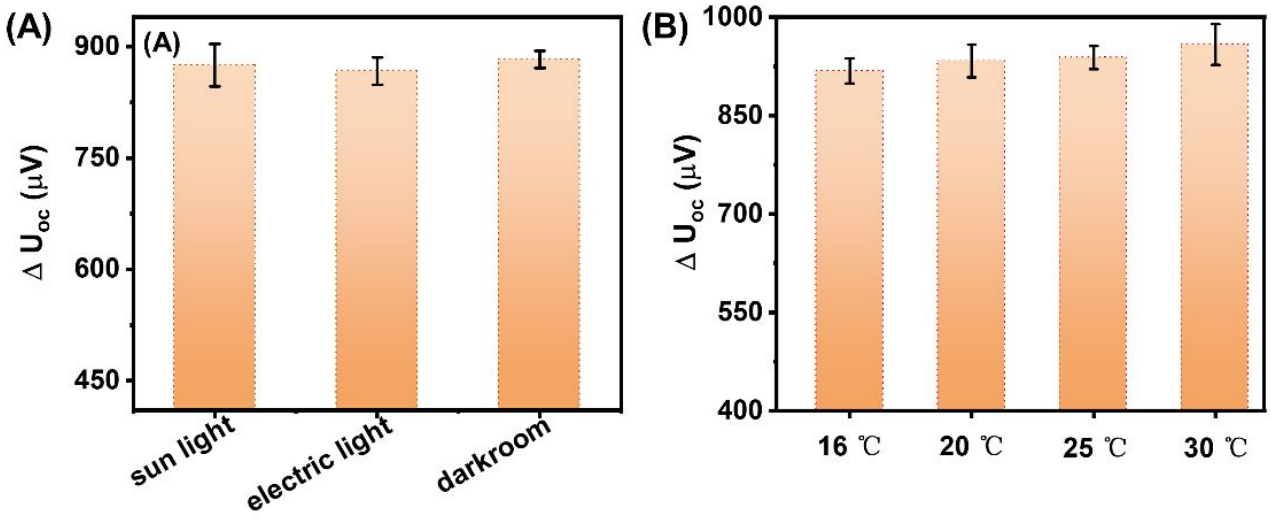

Figure S10. Influence of (A) surrounding light and (B) surrounding temperature.

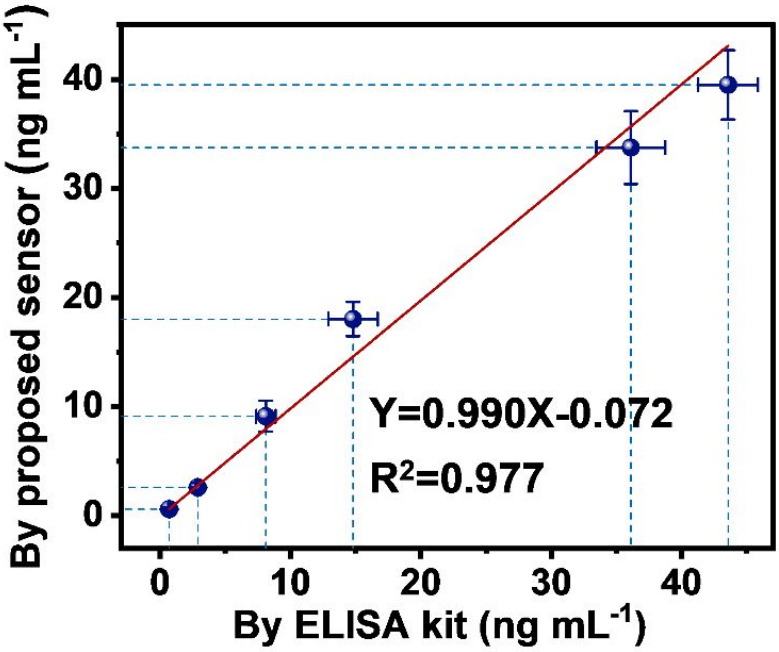

Figure S11. Comparison of the results between the proposed and the referenced AFP ELISA kit.

By using commercialized human AFP ELISA kit as the reference, the accuracy between two methods were performed using a t-test. No significant differences were encountered between these two methods at the 0.05 significance level (Table S1) because all the t_{exp} values in these cases were less than 2.77 ($t_{crit[0.05,4]}$ = 2.77), indicating good accuracy of photothermal-thermoelectric coupled immunoassay with AFP ELISA kit for the analysis of complex biological fluids.

Table S1. Comparison of Different Immunosensing Schemes for the Detection of AFP

detection method	linear range ($ng\ mL^{-1}$)	LOD ($ng\ mL^{-1}$)	Ref.
self-powered electrochromic immunosensor	5.0–2000	1.67	1
SERS-based immunosensor	50–10000	5	2
electrochemical immunosensor	0.4–1000	0.01	3
signal-on PEC immunosensor	0.001 - 1000	0.00031	4
giant magnetoimpedance biosensor	1 – 10	0.001	5
fluorescence resonance energy transfer inhibition assay	800– 45000	410	6
photothermal immunoassay	5.0 – 30	3.8	This work
photothermal-thermoelectric coupled immunoassay	0.5 – 60	0.39	This work

Table S2. Comparison of Analytical Results for Human AFP Serum Samples by Photothermal-Thermoelectric Coupled Immunoassay and Human AFP ELISA Kit

sample no.[a]	method accuracy (Conc.: mean ± SD, ng mL $^{-1}$, n = 3)		t_{exp}
	photothermal-thermoelectric coupled immunoassay	AFP ELISA kit	
1	39.50 ± 3.17	43.57 ± 2.29	1.80
2	33.75 ± 3.34	36.11 ± 2.64	0.96
3	18.02 ± 1.57	14.80 ± 1.89	2.28
4	9.12 ± 1.42	8.10 ± 0.75	1.09
5	2.59 ± 0.41	2.89 ± 0.19	1.13
6	0.60 ± 0.18	0.69 ± 0.06	0.79

[a] Samples 1-3 were 100% human serum, whereas samples 4-6 were acquired by dilution sample 3 to 2-fold, 6-fold and 20-fold, respectively.

REFERENCES

(1) Yu, Z.; Cai, G.; Ren, R.; Tang, D. A new enzyme immunoassay for alpha-fetoprotein in a separate setup coupling an aluminium/Prussian blue-based self-powered electrochromic display with a digital multimeter readout. *Analyst* **2018**, *143*, 2992-2996.

(2) Zhang, C.; Gao, Y.; Yang, N.; You, T.; Chen, H.; Yin, P. Direct determination of the tumor marker AFP via silver nanoparticle enhanced SERS and AFP-modified gold nanoparticles as capturing substrate. *Microchim. Acta* **2018**, *185*, 90.

(3) Wei, T.; Zhang, W.; Tan, Q.; Cui, X.; Dai, Z. Electrochemical assay of the alpha fetoprotein-L3 isoform ratio to improve the diagnostic accuracy of hepatocellular carcinoma. *Anal. Chem*. **2018**, *90*, 13051-13058.

(4) Chen, J.; Zhao, G. A novel signal-on photoelectrochemical immunosensor for detection of alpha-fetoprotein by in situ releasing electron donor. *Biosens. Bioelectron.* **2017**, *98*, 155-160.

(5) Wang, T.; Yang, Z.; Lei, C.; Lei, J.; Zhou, Y. An integrated giant magnetoimpedance biosensor for detection of biomarker. *Biosens. Bioelectron.* **2014**, *58*, 338-344.

(6) Wu, B.; Wang, H.; Chen, J.; Yan, X. Fluorescence resonance energy transfer inhibition assay for α-fetoprotein excreted during cancer cell growth using functionalized persistent luminescence nanoparticles. *J. Am. Chem. Soc.* **2010**, *133*, 686-688.

SUPPORTING VIDEO CAPTION

Video S1. The response of the thermoelectric module for hot water.